Nanoscale Research Letters
a SpringerOpen Journal

NANO EXPRESS Open Access

# Microwave fabrication of $Cu_2ZnSnS_4$ nanoparticle and its visible light photocatalytic properties

Zhihua Zhou†, Pingan Zhang†, Yuelai Lin, Eric Ashalley, Haining Ji, Jiang Wu, Handong Li and Zhiming Wang*

**Abstract**

$Cu_2ZnSnS_4$ nanoparticle with an average diameter of approximately 31 nm has been successfully synthesized by a time effective microwave fabrication method. The crystal structure, surface morphology, and microstructure of the $Cu_2ZnSnS_4$ nanoparticle were characterized. Moreover, the visible light photocatalytic ability of the $Cu_2ZnSnS_4$ nanoparticle toward degradation of methylene blue (MB) was also studied. About 30% of MB was degraded after 240 min irradiation when employing $Cu_2ZnSnS_4$ nanoparticle as a photocatalyst. However, almost all MB was decomposed after 90 min irradiation when introducing a small amount of $H_2O_2$ as a co-photocatalyst. The enhancement of the photocatalytic performance was attributed to the synergetic effect between the $Cu_2ZnSnS_4$ nanoparticle and $H_2O_2$. The detailed photocatalytic degradation mechanism of MB by the $Cu_2ZnSnS_4$ was further proposed.

**Keywords:** $Cu_2ZnSnS_4$; Microwave fabrication; Photocatalyst

## Background

Organic dyes widely used in textile and plastic industries are one of the chief sources of contaminants in wastewater. They have induced serious environmental problems due to their potential toxicity to living organisms. Degradation and total removal of such contaminants are keys to ensuring a protected environment. A photocatalytic technique is considered to be a promising method for treating organic dyes in wastewater [1]. However, an obvious challenge for degradation of organic dyes is that most photocatalysts, such as $TiO_2$ or $BiVO_4$ [2,3], are only effective in the UV range. To broaden their light absorption range, various methods including dye sensitizing [4], metal doping [5] non-metal doping [6,7], and noble metal decorating [8] have been developed. However, stable and efficient dyes are rare and expensive. Moreover, dopant impurity atoms in photocatalysts often serve as recombination centers for photogenerated holes and electrons [9]. To avoid these problems, great efforts have also been put into the development of alternative undoped photocatalysts which work under visible light irradiation. Until now, many materials with attractive visible light photocatalytic performance, such as $Bi_2TiO_4F_2$ [10], $Bi_2O_3$ [11], $AgNbO_3$ [12], and graphene oxide enwrapped Ag/AgX (X = Br, Cl) nanocomposite [13] have been investigated. However, the supply of rare elements of Ag, Bi, and Nb is a critical issue for widespread use. Thus, it is crucial to investigate alternative cost-effective visible-light-driven photocatalysts.

$Cu_2ZnSnS_4$ is a direct bandgap p-type semiconductor with a high optical absorption coefficient of about $10^5$ $cm^{-1}$ [14,15]. Its elements are environmentally friendly and abundant in the earth's crust. As its bandgap is around 1.5 eV, it can absorb most of the visible light. It has been reported that $Cu_2ZnSnS_4$ possesses high photocorrosion resistance in air and aqueous solution [16]. Both of these superior properties of $Cu_2ZnSnS_4$ enrich its potential use in solar-energy-related applications.

In this work, we have fabricated the $Cu_2ZnSnS_4$ nanoparticle by a facile microwave fabrication method. The advantages of this method are the following: it is economical of time and cost effective. The crystal structure and surface morphology of the prepared $Cu_2ZnSnS_4$ nanoparticle were characterized. Moreover, the photocatalytic performance of the $Cu_2ZnSnS_4$ nanoparticle toward the degradation of methylene blue (MB) under visible light irradiation was also investigated. The $Cu_2ZnSnS_4$ nanoparticle showed noteworthy visible light photocatalytic ability.

* Correspondence: zhmwang@gmail.com
†Equal contributors
State Key Laboratory of Electronic Thin Films and Integrated Devices, School of Microelectronics and Solid-State Electronics, University of Electronic Science and Technology of China, Chengdu 610054, P. R. China

## Methods

The $Cu_2ZnSnS_4$ nanoparticle was synthesized by a facile microwave fabrication method. $Cu(CH_3COO)_2 \cdot H_2O$, $Zn(CH_3COO)_2$, $Sn(CH_3COO)_2$, and thiocarbamide with a molar ratio of 2:1:1:4 were employed as source materials. All the reagents were analytically pure and bought from Sinopharm Chemical Reagent Co., Ltd, Shanghai, China. Typically, 1.123 g of the source materials was dissolved in 20 mL ethylene glycol solution as precursor. Then the precursor was stirred gently and heated in a microwave reactor (MCR-3, Gongyi City Yuhua Instrument Co., Ltd, Gongyi City, China) at 180°C for 10 min. After the vacuum filtration and drying process, the $Cu_2ZnSnS_4$ nanoparticle sample was obtained.

The crystal structure of the $Cu_2ZnSnS_4$ nanoparticle was investigated by X-ray diffraction (XRD; D/max-2200/PC, Rigaku, Tokyo, Japan) and Raman spectroscopy (Senterra, Bruker, Billerica, USA). The surface morphology and microstructure of the $Cu_2ZnSnS_4$ were measured by scanning electron microscopy (SEM; JSM 5800LV, JEOL, Tokyo, Japan) and transmission electron microscopy (TEM; JEM-2100, JEOL, Tokyo, Japan).

The photocatalytic properties of the prepared $Cu_2ZnSnS_4$ nanoparticle were investigated by employing MB as a model dye. The $Cu_2ZnSnS_4$ nanoparticle (20 mg) was dispersed in 100 mL of MB aqueous solution (10 mg/L). Prior to irradiation, the MB solution over the catalyst was gently stirred in the dark for 30 min to reach equilibrium adsorption state. Then the solution was illuminated with a 100-W xenon light source (Shanghai Yaming Lighting Co., Ltd., Shanghai, China). The concentration change of MB was monitored by measuring UV-vis absorption of the extracted MB solution at regular intervals. The characteristic peak absorbance of MB at 665 nm was used to determine its concentration. In addition, the photocatalytic properties of the $Cu_2ZnSnS_4$ nanoparticle with the assistance of 0.1 mL $H_2O_2$ (30% aqueous solution) were further investigated in the same measurement process. For comparison, a control experiment without adding $Cu_2ZnSnS_4$ and $H_2O_2$ was also carried out.

## Results and discussion

The crystal structure of the prepared $Cu_2ZnSnS_4$ nanoparticle is shown in Figure 1. The observed diffraction peaks at $2\theta = 28.48°$, 32.77°, 47.38°, and 56.26° correspond to the $Cu_2ZnSnS_4$ crystal planes (112), (200), (220), and (312), which match well with the standard XRD data file of $Cu_2ZnSnS_4$ (JCPDS No. 26-0575). No other crystalline by-products were observed in the pattern, suggesting that the as-prepared sample was pure $Cu_2ZnSnS_4$. Additionally, the strong relative intensity of the (112) and (220) lines indicates the $Cu_2ZnSnS_4$ nanoparticle is preferentially oriented in the (200) and (110) directions during the growing process.

In addition, it has been reported that the spectra of $Cu_2ZnSnS_4$ and β-ZnS are very similar in the XRD

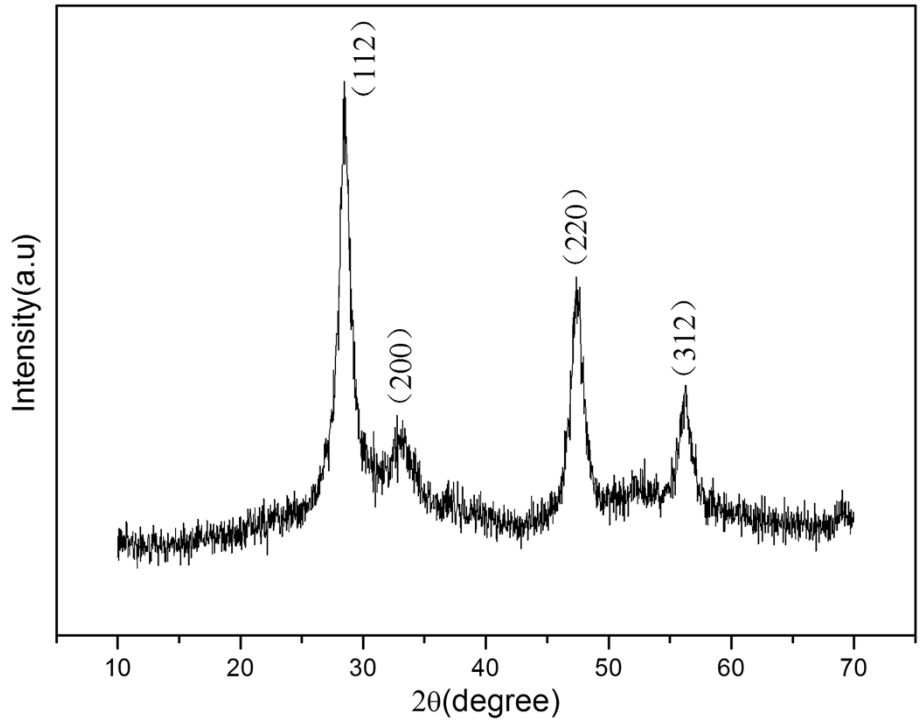


**Figure 1 XRD pattern for the $Cu_2ZnSnS_4$ nanoparticle.** The peaks have been indexed to kesterite $Cu_2ZnSnS_4$ (JCPDS No. 26-0575).

analysis results [17]. Raman spectroscopy analysis is a feasible method to distinguish $Cu_2ZnSnS_4$ from β-ZnS [18]. Therefore, we employed Raman spectroscopy to further confirm the structure of the prepared $Cu_2ZnSnS_4$ nanoparticle. A Raman spectrum of the prepared $Cu_2ZnSnS_4$ nanoparticle over the wave number range of 200 to 450 $cm^{-1}$ is shown in Figure 2. There is an intensive peak located at approximately 331 $cm^{-1}$, which suggests the existence of $Cu_2ZnSnS_4$ [17,19]. The characteristic peaks of β-ZnS located at 348 and 356 $cm^{-1}$ are not observed in the spectrum [20], indicating the absence of β-ZnS.

Surface morphology and microstructure of inorganic semiconductor materials are of vital importance to their optoelectronic properties. Accordingly, the surface morphology of the $Cu_2ZnSnS_4$ nanoparticle was studied by SEM. Figure 3a demonstrates a representative surface morphology of the $Cu_2ZnSnS_4$ nanoparticle. It can be seen that the $Cu_2ZnSnS_4$ nanoparticle possesses similar sizes in diameter and packs uniformly. The average diameter of the $Cu_2ZnSnS_4$ nanoparticle is approximately 31 nm calculated from randomly selected 100 nanoparticles. High-resolution transmission electron microscopy (HRTEM) was further employed to investigate the microstructure of the $Cu_2ZnSnS_4$ nanoparticle. Figure 3b shows a typical HRTEM image of the $Cu_2ZnSnS_4$ nanoparticle. The interplanar spacing of 2.7 Å corresponds to the (200) plane of kesterite $Cu_2ZnSnS_4$. The selected area electron diffraction (SAED) pattern shown in Figure 3c suggests the polycrystalline nature of the nanoparticle.

To evaluate the photocatalytic performance, we analyzed the decomposition of the (MB) dye in aqueous solution over the $Cu_2ZnSnS_4$ nanoparticle under visible light irradiation. Figure 4a presents the time-dependent absorption spectra of MB degradation over the $Cu_2ZnSnS_4$ nanoparticle upon visible light irradiation. The five curves in the pattern are the UV-vis spectra of MB solutions extracted at 0 min, 30 min, 60 min, 150 min, and 240 min. It can be observed that the absorbance peak at 665 nm, which is the characteristic absorption peak of MB, reduced slowly with increasing irradiation time. After 240 min, only about 30% of MB was degraded. In addition, it was difficult to further degrade MB by increasing the irradiation time. However, with the addition of 0.1 mL $H_2O_2$ (30% aqueous solution), as shown in Figure 4c, almost all MB was degraded after 90 min irradiation. In general, peroxymonosulfate, peroxydisulfate, and $H_2O_2$ are often employed to assist in evaluating the photocatalytic properties of semiconductor materials. Both peroxymonosulfate and peroxydisulfate can be driven by visible light for photochemical oxidation [21], while $H_2O_2$ can hardly be activated [22]. Additionally, as a typical organic pollutant, MB is stable under visible light irradiation if no photocatalysts are involved. Therefore, the degradation of MB molecules was attributed to the synergetic effect of $Cu_2ZnSnS_4$ nanoparticle and $H_2O_2$. The $H_2O_2$ enhanced the photocatalytic ability through an

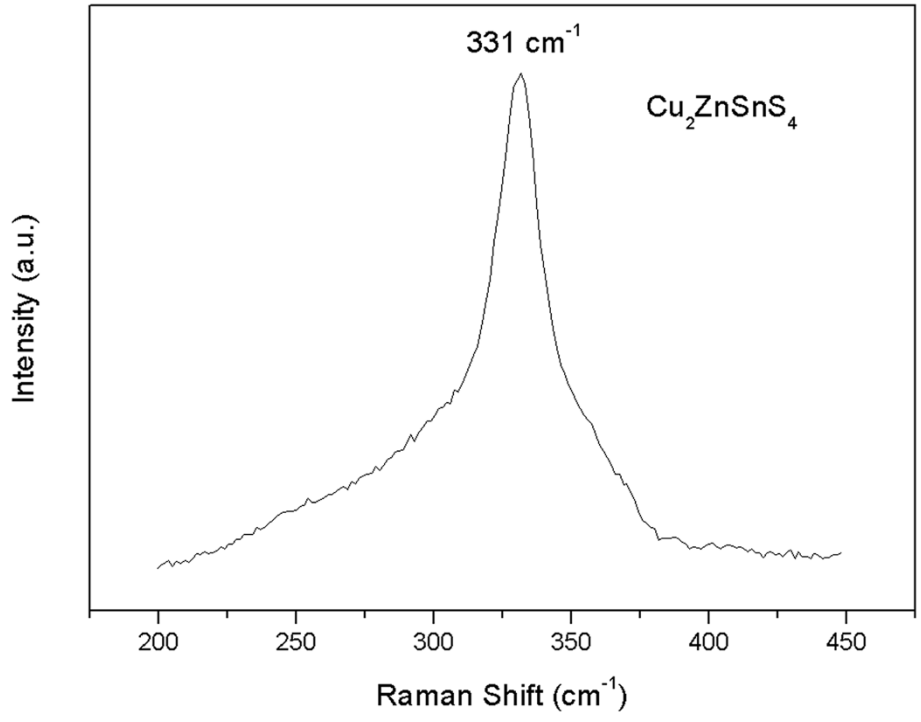


**Figure 2** Raman spectra of the prepared $Cu_2ZnSnS_4$ nanoparticle.

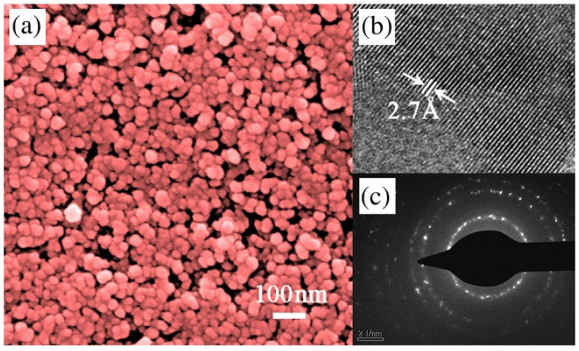


**Figure 3 SEM, HRTEM, and SAED images of the prepared $Cu_2ZnSnS_4$ nanoparticle. (a)** Scanning electron microscopy (SEM), **(b)** high-resolution transmission electron microscopy (HRTEM), and **(c)** selected area electron diffraction (SAED) images of the prepared $Cu_2ZnSnS_4$ nanoparticle.

efficient charge transfer of the photogenerated carriers from the surface of the $Cu_2ZnSnS_4$ nanoparticle to the MB molecule. Figure 4b,d illustrates the curves of $C/C_0$, where $C_0$ is the initial concentration of MB and $C$ is the concentration of MB at time $t$. Insets in Figure 4b,d present the curve of the corresponding $\ln(C_0/C)$ versus irradiation time. No linear relationship between irradiation time and $\ln(C_0/C)$ can be observed when employing the $Cu_2ZnSnS_4$ as a photocatalyst solely. However, with the assistance of $H_2O_2$, a linear relationship between irradiation time and $\ln(C_0/C)$ is well established, suggesting that the photodegradation of MB over the $Cu_2ZnSnS_4$ nanoparticle and $H_2O_2$ proceeded through the pseudo-first-order kinetic reaction [23]. The first-order reaction rate constant $k_1$ was 0.04 $min^{-1}$, which is comparable to that of $TiO_2$-C hybrid aerogel photocatalysts ($0.01 \sim 0.06\ min^{-1}$) toward the degradation of MB driven by UV light irradiation [24].

According to the experiment results and previous reports, the photocatalytic degradation mechanism by the $Cu_2ZnSnS_4$ nanoparticle under visible light irradiation was illustrated in Figure 5 and proposed as follows:

$$Cu_2ZnSnS_4 \xrightarrow{\text{visible light}} Cu_2ZnSnS_4\left(e_{cb}^- + h_{vb}^+\right) \quad (1)$$

When the photogenerated carriers emigrate to the surface of the $Cu_2ZnSnS_4$ nanoparticle, the generated $Cu_2ZnSnS_4\left(h_{vb}^+\right)$ provides holes, decomposing the absorbed contaminant.

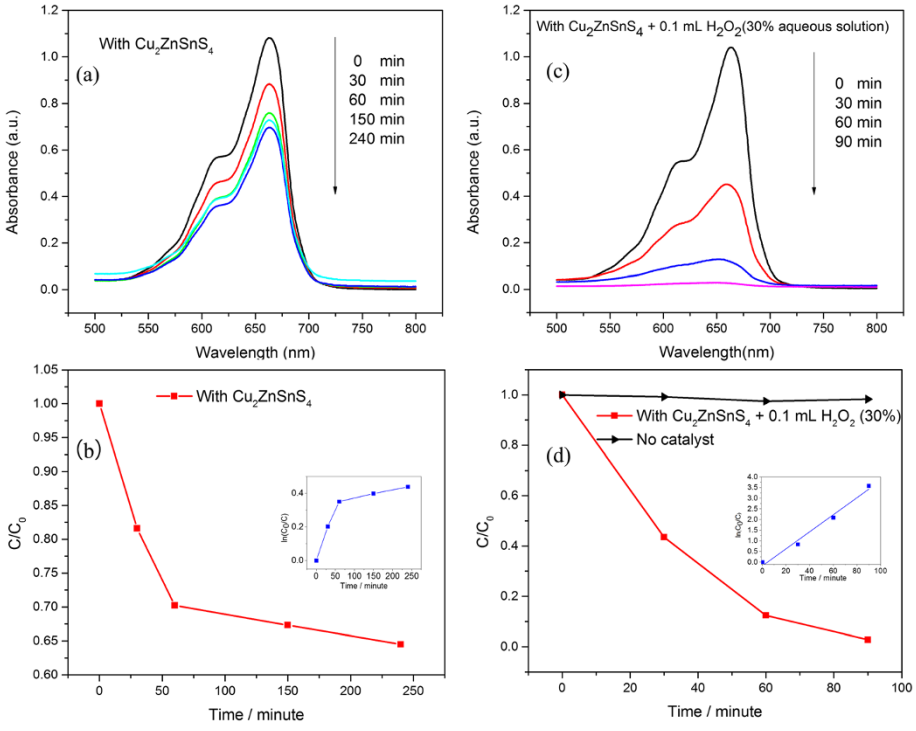


**Figure 4 Photocatalytic activity of the $Cu_2ZnSnS_4$ nanoparticle toward the photodegradation of methylene blue (MB). (a)** Time-dependent UV-vis absorbance spectra of the MB solution using the prepared $Cu_2ZnSnS_4$ nanoparticle as a photocatalyst. **(b)** Curves of the degradation rate of the MB dye with the prepared $Cu_2ZnSnS_4$ nanoparticle ($C_0$ is the initial concentration of MB; $C$ is the reaction concentration of MB at time $t$). The inset shows the $\ln(C_0/C)$ versus time curve of the photodegradation of MB. **(c)** Time-dependent UV-vis absorbance spectra of the MB solution using the prepared $Cu_2ZnSnS_4$ nanoparticle and 0.1 mL $H_2O_2$ as photocatalysts. **(d)** Curves of the degradation rate of the MB dye with the prepared $Cu_2ZnSnS_4$ nanoparticle and 0.1 mL $H_2O_2$ as photocatalysts. The inset presents the $\ln(C_0/C)$ versus time curve of the photodegradation of MB.

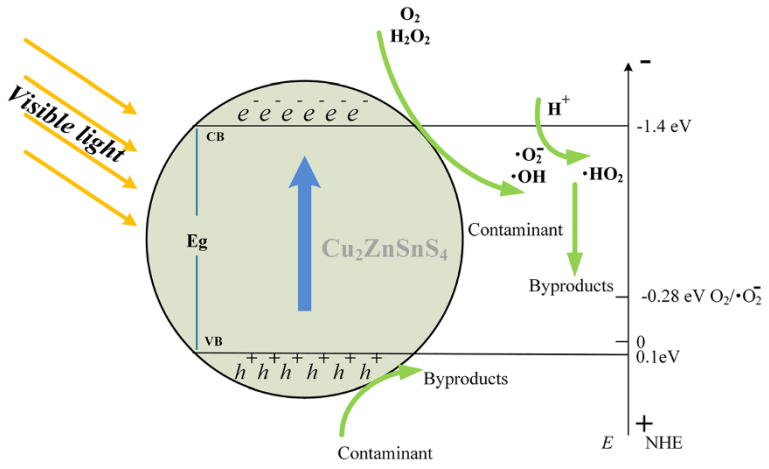


**Figure 5 Schematic diagram for charge carrier separation and photocatalytic contaminant decomposition on $Cu_2ZnSnS_4$ photocatalyst under visible light irradiation.**

$$Cu_2ZnSnS_4\left(h^+_{vb}\right) + \text{contaminant} \rightarrow \text{degraded products} \quad (2)$$

However, due to the top of the valence band of $Cu_2ZnSnS_4$ (+0.1 eV versus NHE) is lower than those of $\cdot OH/H_2O$ (+2.27 eV) and $\cdot OH/OH^-$ (+1.99 eV), the $Cu_2ZnSnS_4$ nanoparticle cannot further degrade the MB with increasing the irradiation time. More recently, Yu *et al.* [25] have reported that a noble metal such as Au or Pt can greatly improve the photocatalytic ability of the $Cu_2ZnSnS_4$ nanoparticle. The enhancement is attributed to surface plasmon resonance (SPR) effect, which can notably reduce the carrier recombination rate on the surface of the $Cu_2ZnSnS_4$ nanoparticle. In our work, with the addition of a small amount of $H_2O_2$, the generated $Cu_2ZnSnS_4$ $\left(e^-_{cb}\right)$ can react with the added $H_2O_2$, generating $\cdot OH$, and subsequently photodegrade the absorbed contaminant.

$$H_2O_2(\text{added}) + Cu_2ZnSnS_4\left(e^-_{cb}\right) \rightarrow \cdot OH + OH^- \quad (3)$$

$$\cdot OH + \text{contaminant} \rightarrow \text{degraded products} \quad (4)$$

$H_2O_2$, as an efficient electron scavenger and a source of $\cdot OH$ with high oxidizing ability, was added here to assist the photodegradation of the contaminant. However, an excess amount of $H_2O_2$ will decrease the photocatalytic activity [26]. As shown in Equation 5, the excess $H_2O_2$ scavenges the beneficial OH generating a much weaker hyperoxyl radical of $HO^{\bullet}_2$.

$$H_2O_2 + \cdot OH \rightarrow HO^{\bullet}_2 + H_2O \quad (5)$$

Besides, the $HO^{\bullet}_2$ will further react with the remaining $\cdot OH$ forming ineffective oxygen and water.

$$HO^{\bullet}_2 + \cdot O \rightarrow H_2O + O_2 \quad (6)$$

## Conclusions

In summary, the $Cu_2ZnSnS_4$ nanoparticle was successfully synthesized by a facile microwave fabrication method. The prepared $Cu_2ZnSnS_4$ nanoparticle exhibited a polycrystalline structure with an average diameter of approximately 31 nm. The photocatalytic performance of the $Cu_2ZnSnS_4$ nanoparticle toward degradation of MB in aqueous solution was also investigated. Due to the top of the valence band of $Cu_2ZnSnS_4$, pure $Cu_2ZnSnS_4$ nanoparticle showed a poor visible light photocatalytic ability. However, when employing a small amount of $H_2O_2$ as electron scavenger, the photocatalytic performance was greatly enhanced. The first-order reaction rate constant $k_1$ toward the degradation MB reached as high as 0.04 $min^{-1}$. The synergetic effect between the $Cu_2ZnSnS_4$ nanoparticle and $H_2O_2$ was a key to promote the photodegradation efficiency.

### Competing interests

The authors declare that they have no competing interests.

### Authors' contributions

ZHZ formulated the idea of investigation and drafted the manuscript. PAZ prepared the $Cu_2ZnSnS_4$ nanoparticles. YLL and AE have taken part in acquisition and interpretation of data. HNJ, JW, and HDL directed the research and made corrections to the manuscript. ZMW supervised the study. All authors have read and approved the final manuscript.

**Acknowledgements**
This work was supported by the Fundamental Research Funds for the Central Universities 2672012ZYGX2012J042, the 973 Program (2013CB933800), and the National Natural Science Foundation of China (51272038).

Received: 22 August 2014 Accepted: 2 September 2014
Published: 9 September 2014

**References**

1. Liao J, Lin S, Zhang L, Pan N, Cao X, Li J: **Photocatalytic degradation of methyl orange using a $TiO_2$/Ti mesh electrode with 3D nanotube arrays.** *ACS Appl Mater Interfaces* 2011, **4:**171–177.
2. Ding D, Long M, Cai W, Wu Y, Wu D, Chen C: **In-situ synthesis of photocatalytic $CuAl_2O_4$-Cu hybrid nanorod arrays.** *Chem Commun* 2009, **24:**3588–3590.
3. Chandrappa KG, Venkatesha TV, Sharifah BAH: **Electrochemical generation of cubic shaped nano $Zn_2SnO_4$ photocatalysts.** *Nano Micro Letters* 2013, **5:**101–110.
4. Hsiao Y-C, Wu T-F, Wang Y-S, Hu C-C, Huang C: **Evaluating the sensitizing effect on the photocatalytic decoloration of dyes using anatase-$TiO_2$.** *Appl Catal B Environ* 2014, **148–149:**250–257.
5. De Trizio L, Buonsanti R, Schimpf AM, Llordes A, Gamelin DR, Simonutti R, Milliron DJ: **Nb-doped colloidal $TiO_2$ nanocrystals with tunable infrared absorption.** *Chem Mater* 2013, **25:**3383–3390.
6. Zhang Z, Luo Z, Yang Z, Zhang S, Zhang Y, Zhou Y, Wang X, Fu X: **Band-gap tuning of N-doped $TiO_2$ photocatalysts for visible-light-driven selective oxidation of alcohols to aldehydes in water.** *RSC Advances* 2013, **3:**7215–7218.
7. Chen C, Cai W, Long M, Zhou B, Wu Y, Wu D, Feng Y: **Synthesis of visible-light responsive graphene oxide/$TiO_2$ composites with p/n heterojunction.** *ACS Nano* 2010, **4:**6425–6432.
8. Zhang J, Chen G, Chaker M, Rosei F, Ma D: **Gold nanoparticle decorated ceria nanotubes with significantly high catalytic activity for the reduction of nitrophenol and mechanism study.** *Appl Catal B Environ* 2013, **132–133:**107–115.
9. Gai Y, Li J, Li S-S, Xia J-B, Wei S-H: **Design of narrow-gap $TiO_2$: a passivated codoping approach for enhanced photoelectrochemical activity.** *Phys Rev Lett* 2009, **102:**036402.
10. Jiang B, Zhang P, Zhang Y, Wu L, Li HX, Zhang DQ, Li GS: **Self-assembled 3D architectures of $Bi_2TiO_4F_2$ as a new durable visible-light photocatalyst.** *Nanoscale* 2012, **4:**455–460.
11. Sajjad S, Leghari SAK, Zhang JL: **Nonstoichiometric $Bi_2O_3$: efficient visible light photocatalyst.** *Rsc Advances* 2013, **3:**1363–1367.
12. Wu W, Liang S, Chen Y, Shen L, Yuan R, Wu L: **Mechanism and improvement of the visible light photocatalysis of organic pollutants over microcrystalline $AgNbO_3$ prepared by a sol–gel method.** *Mater Res Bull* 2013, **48:**1618–1626.
13. Zhu MS, Chen PL, Liu MH: **Graphene oxide enwrapped Ag/AgX (X = Br, Cl) nanocomposite as a highly efficient visible-light plasmonic photocatalyst.** *ACS Nano* 2011, **5:**4529–4536.
14. Chen S, Walsh A, Gong X-G, Wei S-H: **Classification of lattice defects in the kesterite $Cu_2ZnSnS_4$ and $Cu_2ZnSnSe_4$ earth-abundant solar cell absorbers.** *Adv Mater* 2013, **25:**1522–1539.
15. Xinkun W, Wei L, Shuying C, Yunfeng L, Hongjie J: **Photoelectric properties of $Cu_2ZnSnS_4$ thin films deposited by thermal evaporation.** *J Semicond* 2012, **33:**022002.
16. Wang L, Wang W, Sun S: **A simple template-free synthesis of ultrathin $Cu_2ZnSnS_4$ nanosheets for highly stable photocatalytic $H_2$ evolution.** *J Mater Chem* 2012, **22:**6553–6555.
17. Fernandes PA, Salome PMP, da Cunha AF: **Growth and Raman scattering characterization of $Cu_2ZnSnS_4$ thin films.** *Thin Solid Films* 2009, **517:**2519–2523.
18. Fernandes PA, Salomé PMP, da Cunha AF: **Study of polycrystalline $Cu_2ZnSnS_4$ films by Raman scattering.** *J Alloy Compd* 2011, **509:**7600–7606.
19. Zou C, Zhang LJ, Lin DS, Yang Y, Li Q, Xu XJ, Chen X, Huang SM: **Facile synthesis of $Cu_2ZnSnS_4$ nanocrystals.** *Crystengcomm* 2011, **13:**3310–3313.
20. Serrano J, Cantarero A, Cardona M, Garro N, Lauck R, Tallman RE, Ritter TM, Weinstein BA: **Raman scattering in beta -ZnS.** *Phys Rev B* 2004, **69:**014301.
21. Zhou G, Sun H, Wang S, Ming Ang H, Tadé MO: **Titanate supported cobalt catalysts for photochemical oxidation of phenol under visible light irradiations.** *Sep Purif Technol* 2011, **80:**626–634.
22. Sun H, Liu S, Liu S, Wang S: **A comparative study of reduced graphene oxide modified $TiO_2$, ZnO and $Ta_2O_5$ in visible light photocatalytic/photochemical oxidation of methylene blue.** *Appl Catal B Environ* 2014, **146:**162–168.
23. Mohamed MM, Al-Esaimi MM: **Characterization, adsorption and photo-catalytic activity of vanadium-doped $TiO_2$ and sulfated $TiO_2$ (rutile) catalysts: degradation of methylene blue dye.** *J Mol Catal A Chem* 2006, **255:**53–61.
24. Shao X, Lu W, Zhang R, Pan F: **Enhanced photocatalytic activity of $TiO_2$-C hybrid aerogels for methylene blue degradation.** *Sci Rep* 2013, **3:**3018.
25. Yu X, Shavel A, An X, Luo Z, Ibáñez M, Cabot A: **$Cu_2ZnSnS_4$-Pt and $Cu_2ZnSnS_4$-Au heterostructured nanoparticles for photocatalytic water splitting and pollutant degradation.** *J Am Chem Soc* 2014, **136:**9236–9239.
26. Shang M, Wang W, Sun S, Ren J, Zhou L, Zhang L: **Efficient visible light-induced photocatalytic degradation of contaminant by spindle-like PANI/$BiVO_4$.** *J Phys Chem C* 2009, **113:**20228–20233.

doi:10.1186/1556-276X-9-477
**Cite this article as:** Zhou *et al.*: Microwave fabrication of $Cu_2ZnSnS_4$ nanoparticle and its visible light photocatalytic properties. *Nanoscale Research Letters* 2014 **9**:477.